*Published in : ASC Applied Polymer Materials (2020), vol. 2, n°2, pp. 922–931*
*DOI: 10.1021/acsapm.9b01130*
*Status : Postprint (Author's version)*

# INFLUENCE OF THE CYCLIC VERSUS LINEAR CARBONATE SEGMENTS IN THE PROPERTIES AND PERFORMANCE OF $CO_2$-SOURCED POLYMER ELECTROLYTES FOR LITHIUM BATTERIES

Farid Ouhib[#], Leire Meabe[#], Abdelfattah Mahmoud, Bruno Grignard, Jean-Michel Thomassin, Frederic Boschini, Haijin Zhu, Maria Forsyth, David Mecerreyes,* and Christophe Detrembleur*

*Farid Ouhib – Centre for Education and Research on Macromolecules (CERM), CESAM Research Unit, University of Liege, Quartier Agora 4000, Liege, Belgium*

*Leire Meabe – POLYMAT, University of the Basque Country UPV/EHU, 20018 Donostia-San Sebastian, Spain*

*Abdelfattah Mahmoud – GREENMAT-LCIS, Chemistry Department, University of Liege, Quartier Agora 4000, Liege, Belgium;*

*Bruno Grignard – Centre for Education and Research on Macromolecules (CERM), CESAM Research Unit, University of Liege, Quartier Agora 4000, Liege, Belgium*

*Jean-Michel Thomassin – Centre for Education and Research on Macromolecules (CERM), CESAM Research Unit, University of Liege, Quartier Agora 4000, Liege, Belgium*

*Frederic Boschini – GREENMAT-LCIS, Chemistry Department, University of Liege, Quartier Agora 4000, Liege, Belgium*

*Haijin Zhu – Institute for Frontier Materials (IFM), Deakin University, Waurn Ponds, VIC 3216, Australia*

*Maria Forsyth – Institute for Frontier Materials (IFM), Deakin University, Waurn Ponds, VIC 3216, Australia; Ikerbasque, Basque Foundation for Science, E-48011 Bilbao, Spain;*

*David Mecerreyes – POLYMAT, University of the Basque Country UPV/EHU, 20018 Donostia-San Sebastian, Spain;*

*Christophe Detrembleur – Centre for Education and Research on Macromolecules (CERM), CESAM Research Unit, University of Liege, Quartier Agora 4000, Liege, Belgium;*

**Abstract**

Polycarbonates bearing linear carbonate linkages and polyether segments have demonstrated to be highly attractive solid electrolyte candidates for the design of safe energy storage devices, for example, lithium metal batteries. In this contribution, we are studying the influence of the introduction of some cyclic carbonate linkages within the polymer backbone on the electrolyte properties. We first describe the synthesis of polycarbonates/polyethers containing different contents of both linear and cyclic carbonate linkages within the chain by the copolymerization of a highly reactive $CO_2$-based monomer (bis(α-alkylidene cyclic carbonate)) with poly(ethylene glycol) diol and a dithiol at room temperature. We then explore the influence of the content of the cyclic carbonates and the loading of the polymer by lithium bis(trifluoromethane) sulfonimide (LiTFSI) on the electrolyte properties (glass transition and melting temperatures, ion conductivity, and diffusivity). The best electrolyte candidate is characterized by a linear/cyclic carbonate linkage ratio of 82/18 when loaded with 30 wt % LiTFSI. It exhibits an ion

*Published in : ASC Applied Polymer Materials (2020), vol. 2, n°2, pp. 922–931*
*DOI: 10.1021/acsapm.9b01130*
*Status : Postprint (Author's version)*

conductivity of $5.6 \times 10^{-5}$ S cm$^{-1}$ at 25 °C ($7.9 \times 10^{-4}$ S cm$^{-1}$ at 60 °C), which surpasses by 150% (424% at 60 °C) the conductivity measured for a similar polymer bearing linear carbonate linkages only. It is also characterized by a high oxidation stability up to 5.6 V (vs Li/Li$^+$). A self-standing membrane is then constructed by impregnating a glass fiber filter by this optimal polymer, LiTFSI, and a small amount of a plasticizer (tetraglyme). Cells are then assembled by sandwiching the membrane between a C-coated $LiFePO_4$ (LFP) as the cathode and lithium as the anode and counter electrode. The cycling performances are evaluated at 0.1 C at 60 °C and room temperature for 40 cycles. Excellent cycling performances are noted with 100% of the theoretical capacity (170 mAh g$^{-1}$) at 60 °C and 73.5% of the theoretical capacity (125 mAh g$^{-1}$) at 25 °C.

**Keywords:**

Polycarbonate, polymer electrolyte, carbon dioxide, ion conductivity, solid electrolyte, cyclic carbonate, lithium battery

# Introduction

A promising way to store energy in a more secure fashion consists in developing flexible and lightweight batteries that contain solid polymer electrolytes (SPEs). Poly(ethylene oxide) (PEO)-based SPEs are currently the most important ones due to many attributes (good solvation of many salts, high thermal stability, good mechanical properties and compatibility with metal electrodes, and high ion conductivity at high temperature).[1–4] The lithium transference number (approximately 0.2) and the electrochemical window (4.5 V) of PEO-based SPEs are however low to moderate,[5] limiting the performances of the final device. This search for new polymer electrolyte materials is crucial nowadays due to the need of increasing the power of the batteries by using lithium metal anodes and high voltage cathodes, which requires both higher lithium transfer numbers and electrochemical window. In the last few years, alternative chemistries for polymer electrolytes have been investigated, including polycarbonates, polynitriles, polyalcohols, or polyamines.[6]

In particular, carbonate-containing aliphatic linear polymers have demonstrated excellent electrochemical properties. The high lithium transference number (~0.5) and broader electrochemical stability (4.5–5 V) results[7–10] clearly demonstrate the enhanced properties with respect to PEO-based SPEs (<0.2, <4 V respectively). Moreover, in most of the developed examples the linear polycarbonates are amorphous, whereas PEO is semicrystalline, which hinders the ionic conductivity below the melting temperature of ethylene oxide units, <60 °C.[11,12] The design of all-solid-state lithium batteries that are operating at room temperature can therefore now be envisioned.[10] All these refinements in electrochemical properties are mainly due to the weak coordination between the lithium cation and carbonyl group which helps to dissociate the Li salt and favor the lithium transport.[7,13]

Nowadays, in almost all of the successful works, the carbonate groups are included in the form of linear carbonates in the polymer backbone.[6] Five member cyclic carbonates such as propylene carbonate are commonly used as solvents in organic electrolytes and known to have a high dielectric constant and favorable interactions with lithium salts. However, polymers where the cyclic carbonates are included are usually rigid showing high glass transition temperature ($T_g$) although showing decent ionic

*Published in : ASC Applied Polymer Materials (2020), vol. 2, n°2, pp. 922–931*
*DOI: 10.1021/acsapm.9b01130*
*Status : Postprint (Author's version)*

conductivity values of $10^{-7}$ S cm$^{-1}$ at 40 °C with the combination of $LiCF_3SO_3$.[14] Even if this value is high for the rigid host polymer, making the polymer more flexible and including some ester groups was reported as a strategy to increase the conductivity ($10^{-4}$ S cm$^{-1}$ at room temperature).[14] However, to the best of our knowledge there is no study on polymers which mixed both linear and cyclic carbonates linkages in the main chain.

Current trends are to prepare polycarbonates (PCs) from carbon dioxide as a renewable resource.[15,16] Well beyond sustainability concerns, some of the recent strategies of $CO_2$ conversions are indeed able to produce PCs with novel functionalities that demonstrated some potential as solid electrolytes for battery applications.[9] It was recently demonstrated that the introduction of linear carbonate linkages between PEO segments enabled the design of solid electrolytes with a high ionic conductivity.[17]

In this work, we study the influence of the introduction of cyclic carbonate linkages within a polycarbonate/polyether backbone on the thermal properties and ion conductivity of the polymer loaded or not with LiTFSI. The new polymers are prepared by a facile one-pot organocatalyzed polyaddition process involving an activated $CO_2$-based dicyclic carbonate, a poly(ethylene glycol) diol, and a dithiol. We show how to construct a self-standing solid electrolyte, and we evaluate the cycling performance of a cell constructed using Li as the anode, LFP as the cathode material, and our self-standing membrane as both the separator and solid electrolyte. This work therefore illustrates the exploitation of $CO_2$ to produce polymers that contain both linear and cyclic carbonates within the chain and that show great promise as solid electrolytes for lithium batteries.

**Table 1.** Composition and Macromolecular Characteristics of the (Co)polymers

| entry | polymer | cyclic carbonate (mol %)[a] | linear carbonate (mol %)[a] | ether/carbonate linkages[b] | $M_n$ (g/mol) | Đ | $T_g$ (°C) | $T_m$ (°C) |
|---|---|---|---|---|---|---|---|---|
| 1 | P1 | 100 | 0 | 1 | 54 000 | 1.90 | 43 | |
| 2 | P2 | 79 | 21 | 10 | 32 000 | 2.93 | c | 44 |
| 3 | P3 | 59 | 41 | 19 | 63 000 | 3.84 | c | 41 |
| 4 | P4 | 36 | 64 | 29 | 44 000 | 2.59 | c | 41 |
| 5 | P5 | 18 | 82 | 37 | 114 000 | 2.84 | c | 50 |
| 6 | P6 | 0 | 100 | 45 | 49 000 | 1.53 | c | 41 |

[a]Determined by $^1$H NMR analysis of the copolymer in $CDCl_3$. [b]Ether/carbonate linkages states for the ether/(linear + cyclic) carbonate linkages ratio in the copolymer. [c]$T_g$ cannot be determined by conventional DSC.

# EXPERIMENTAL SECTION

**Materials.** Poly(ethylene glycol) ($M_n$ = 4000 g mol$^{-1}$; Aldrich), 2,2′-(ethylenedioxy)diethanethiol (96%; Aldrich), 1,8-diazabicyclo[5.4.0]undec-7-e,e (DBU, 99%; Fluorochem), and lithium bis(trifluoromethane) sulfonimide (99.9%; Solvionic) are used as received. Meso-4,4-dimethyl-5-methylene-1,3dioxolan-2-one (bis$\alpha$CC) was synthesized as reported elsewhere by our group.[18] Whatman glass microfiber filters (16 mm diameter, 53 g/m$^2$, 0.26 mm thickness) were purchased by Aldrich.

**Typical Procedure for the Synthesis of the Polymers.** Synthesis of **P1**. Bis-$\alpha$CC (1 g, 3.937 mmol, 1 equiv) and 2,2′(ethylenedioxy)diethanethiol (717.7 mg, 3.937 mmol, 1 equiv) were solubilized in dry dimethylformamide (DMF) (0.8 mL) in a reaction tube. A solution of 1,8-diazabicyclo-[5.4.0]-7-undecene (DBU) (1 mL (C = 0.2 M in DMF), 0.19 mmol, 0.05 equiv) was added, and the reaction medium

*Published in : ASC Applied Polymer Materials (2020), vol. 2, n°2, pp. 922–931*
*DOI: 10.1021/acsapm.9b01130*
*Status : Postprint (Author's version)*

was stirred at 25 °C for 24 h. The polymer was purified by two successive precipitations in diethyl ether. The purified polymer was dried under vacuum at 60 °C (1.667 g, 97% of yield). The macromolecular characteristics of the polymer are summarized in **Table 1** (entry 1).

Synthesis of **P2**. Bis-αCC (400 mg, 1.574 mmol, 1 equiv), PEG-4000 (1.26 mg, 0.315 mmol, 0.2 equiv), and 2,2'-(ethylenedioxy)diethanethiol (229.5 mg, 1.259 mmol, 0.8 equiv) were solubilized in dry DMF (1.6 mL) in a reaction tube. A solution of DBU (0.4 mL (C = 0.2 M in DMF), 0.08 mmol, 0.05 equiv) was added, and the reaction medium was stirred at 25 °C for 24 h. The polymer was purified by two successive precipitations in diethyl ether. The purified polymer was dried under vacuum at 60 °C (1.814 g, 96% of yield). The macromolecular characteristics of the polymer are summarized in **Table 1** (entry 2).

Synthesis of **P3**. The same protocol as for **P2** was used with the following contents of reagents: Bis-αCC (300mg, 1.181 mmol, 1 equiv), PEG-4000 (1.889 g, 0.472 mmol, 0.4 equiv), 2,2'(ethylenedioxy)diethanethiol (129.2 mg, 0.708 mmol, 0.6 equiv), dry DMF (2 mL), and solution of DBU (0.3 mL (C = 0.2 M in DMF), 0.06 mmol, 0.05 equiv). The purified and dried polymer was obtained with 93% of yield (2.156 g). The macromolecular characteristics are summarized in **Table 1** (entry 3).

Synthesis of **P4**. The same protocol as for **P2** was used with the following contents of reagents: Bis-αCC (200 mg, 0.787 mmol, 1 equiv), PEG-4000 (1.889 g, 0.472 mmol, 0.6 equiv), 2,2'(ethylenedioxy)diethanethiol (57.4 mg, 0.314 mmol, 0.4 equiv), dry DMF (2 mL), and solution of DBU (0.2 mL (C = 0.2 M in DMF), 0.04 mmol, 0.05 equiv). The purified and dried polymer was obtained with 93% yield (1.996 g). The macromolecular characteristics are summarized in **Table 1** (entry 4).

Synthesis of **P5**. The same protocol as for **P2** was used with the following contents of reagents: Bis-αCC (200 mg, 0.787 mmol, 1 equiv), PEG-4000 (2.518 g, 0.629 mmol, 0.8 equiv), 2,2'(ethylenedioxy)diethanethiol (28.7 mg, 0.157 mmol, 0.2 equiv), dry DMF (2.6 mL), and solution of DBU (0.2 mL (C = 0.2 M in DMF), 0.04 mmol, 0.05 equiv). The purified and dried polymer was obtained with 92% yield (2.526 g). The macromolecular characteristics are summarized in **Table 1** (entry 5).

**P6** was prepared as reported in our previous work.[17]

**Preparation of the Solid Electrolyte Membrane.** A solution containing 175 mg of polymer, 63.06 mg of LiTFSI. and 17.5 mg of tetraglyme was prepared in 2.5 mL of acetone. One hundred microliters of this solution was then deposited on the surface of a Whatman glass microfiber filter (16 mm diameter, 53g/m$^2$). The process was repeated two times with 10 min interval between each deposition. The filter paper was then turned back to perform three deposits of 100 µL of the solution on the other surfaces. After the last deposit, the paper filter was dried overnight at RT under vacuum.

The surface and section of the impregnated paper filter was then observed by scanning electron microscopy (QUANTA 600).

**Characterization Methods.** *Nuclear Magnetic Resonance (NMR) Spectroscopy.* $^1$H and $^{13}$C NMR analyses were performed on Bruker Avance 400 MHz spectrometers in $CDCl_3$ at 25 °C in the Fourier transform mode. Sixteen or 64 scans for a $^1$H spectra and 512 or 2048 scans for $^{13}$C spectra were recorded.

*Published in : ASC Applied Polymer Materials (2020), vol. 2, n°2, pp. 922–931*
*DOI: 10.1021/acsapm.9b01130*
*Status : Postprint (Author's version)*

*Gel Permeation Chromatography (GPC)*. Molecular parameters of the polymers (number-average molecular weight, $M_n$, and dispersity, *Đ*) were determined by size exclusion chromatography (SEC) with a Viscotek 305 TDA liquid chromatograph equipped with two PSS SDV linear M columns calibrated with poly(ethylene oxide) standards and a refractive index detector. Tetrahydrofuran (THF) is used as the eluent at 45 °C with a flow rate of 1 mL/min.

*Differential Scanning Calorimetry (DSC)*. Samples (5 mg in a sealed aluminum pan) were analyzed by a PerkinElmer 8500 DSC equipped with an Intracooler III under ultrapure nitrogen flow, and the instrument was calibrated with dodecane, indium, and tin standards. The samples were first heated at a rate of 10 K $min^{-1}$ from 25 to 100 °C and they were left for 3 min at 100 °C to eliminate the influence of thermal history.[24] They were then cooled down to −80 °C at a rate of 10 K $min^{-1}$. Once again, it was heated up until 100 °C at 10 K $min^{-1}$ after waiting during 3 min at −80 °C.

*Attenuated Total Reflectance Fourier Transform Infrared (ATRFTIR) Spectroscopy.* Measurements were conducted on a PerkinElmer Spektrum ATR spectrometer.

*Scanning Electron Microscopy (SEM).* SEM was performed using a 515 Philips scanning electron microscope.

*Ionic Conductivity.* The ionic conductivity was studied by electrochemical alternating current (ac) impedance spectroscopy (EIS) with an Autolab 302N potentiostat galvanostat with a temperature controlled by a Microcell HC station. The polymer/ LiTFSI mixture (thickness = 250 µm) was sandwiched between two stainless steel electrodes (average surface area of the electrode: 0.5026 $cm^2$) and sealed in a Microcell under inert atmosphere. Frequency range of 0.1 MHz to 0.1 Hz and amplitude of 10 mV.

*$Li^+$ and $NTf_2^-$ Diffusivity.* The $Li^+$ and $NTf_2^-$ diffusivity were measured by $^7Li$ and $^{19}F$ pulsed field gradient nuclear magnetic resonance (PFG-NMR) by using a Bruker spectrometer (300 MHz) at room temperature in DMSO-$d_6$. Diffusion measurements were carried out on a 300 MHz Bruker Advance III spectrometer with a Diff50 pulsed field gradient probe and a stimulated echo pulse sequence. Relaxation measurements were carried out on the same hardware with a saturation recovery pulse sequence.

*Electrochemical Stability.* The electrochemical stability of the membranes was analyzed in CR2032 cells between a lithium disk and a stainless steel (SS) electrode by using an Autolab 302N potentiostat galvanostat. The coin cells were first stabilized at 70 °C for 24 h before evaluating their electrochemical stability window by cyclic voltammetry (CV) at 70 °C. The anodic limit was evaluated between open circuit potential (OCV) and 6.0 V versus $Li/Li^+$ at 0.5 mV $s^{-1}$.

*Battery Performances.* The battery performances of the electrolyte membranes were conducted in two-electrode coin cells using Ccoated $LiFePO_4$ (LFP) provided by Prayon-beLife company (Pholicat FE-100) as the working electrode, Li metal (Aldrich) as the counter and reference electrode, and the solid electrolyte membrane. The positive electrode was prepared by dispersing 60 wt % of $LiFePO_4$, 20 wt % conductive carbon (Super P), and 20 wt % of polymer **P5** as the binder in acetone under stirring for 2 h. This slurry, deposited on aluminum foil by the doctor-blade method (thickness: 120 µm), was dried at 50 °C in vacuum for 8 h. Discs (1.2 cm diameter; containing 1−2 mg/$cm^2$ of $LiFePO_4$) were cut. The solid electrolyte consisting of 58.4 wt % **P5**, 21 wt % LiTFSI, 14.8 wt % glass microfiber filter, and 5.8 wt % TEG as prepared above was sandwiched between metallic lithium and the working electrode.

*Published in : ASC Applied Polymer Materials (2020), vol. 2, n°2, pp. 922–931*
*DOI: 10.1021/acsapm.9b01130*
*Status : Postprint (Author's version)*

CR2032 coin cells were assembled under argon atmosphere in the glovebox. The galvanostatic charge/discharge curves were measured between 2.0 and 4.2 V versus $Li^+/Li^0$ at 0.1 C cycling rate (1 Li per f.u. in *n* hours) and under thermostatic conditions (25 ± 0.5 and at 60 ± 1 °C) by using a multichannel Biologic potentiostat (VMP3). Throughout the manuscript, the capacity refers to the mass of $LiFePO_4$ active material in the composite cathode.

*Thermal Stability.* The thermal stability of the **P5** polymer and **P5** loaded with 30 wt % of LiTFSI was evaluated with a TGA2 star$^e$ system from Mettler Toledo using a thermal ramp of 20 °C/min under nitrogen flow.

# RESULTS AND DISCUSSION

**Scheme 1.** Reaction Scheme for the Synthesis of the Polymers Containing Cydic/Linear Carbonate and Ether Liknages[a]

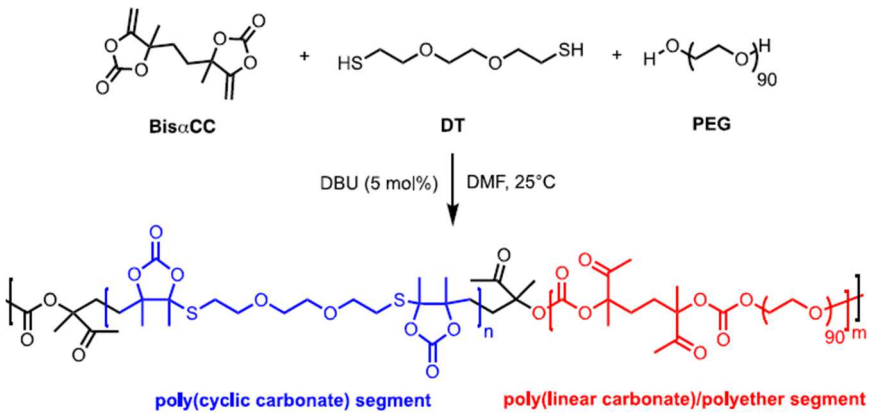


[a]Cyclic carbonate groups can also be alternated with linear ones, however they are not represented for sake of clarity

**Copolymer Synthesis and Characterizations.** The incorporation of the cyclic carbonate moieties within the linear polymer chain is realized by adding a dithiol DT (2,2'(ethylenedioxy)diethanethiol) to the organocatalyzed copolymerization of a bis(α-alkylidene cyclic carbonate) (BisαCC) with polyethylene glycol PEG ($M_n$ = 4000 g/mol) according to a simple one-pot process as illustrated in **Scheme 1**. According to previous works, the ring-opening of BisαCC by PEG provides the linear carbonate units,[17,18] and the addition of the thiol to BisαCC furnishes the cyclic carbonate one substituted by a thioether group.[19] Various contents of cyclic and linear carbonates were targeted in order to ultimately study the influence of the cyclic carbonate units on the material performances. All polymerizations were carried out under identical conditions until full monomer consumption at 25 °C for 24 h by using 5 mol % DBU as a catalyst in DMF. For the sake of comparison, a homopolymer of polycyclic carbonate was prepared according to the same protocol by DBU catalyzed polyaddition of BisαCC with the dithiol DT without PEG following our previously reported strategy.[19] The macromolecular characteristics of the (co)polymers are summarized in **Table 1**.

Although the apparent number-average molar masses ($M_n$) of the copolymers cannot be compared (as they are determined by SEC using a PEO calibration), they are all characterized by reasonable molar masses (32 000−114 000 g/mol) and rather high dispersity in line with a step-growth polymerization

*Published in : ASC Applied Polymer Materials (2020), vol. 2, n°2, pp. 922–931*
*DOI: 10.1021/acsapm.9b01130*
*Status : Postprint (Author's version)*

process. **Figure 1** shows the $^{1}$H NMR spectra of the two homopolymers (**P1** with 100% cyclic carbonates linkages and **P6** with 100% linear ones) and a representative copolymer, **P3**, that contains 59 mol % of cyclic carbonate linkages. The cyclic to linear carbonate content was determined by comparison of the relative intensities of signals related to the methylene attached to the tetrasubstituted ethylene carbonate moiety via the thioether linkage (−$CH_2$− S−, $\delta$ = 2.95 ppm) and the methylene adjacent to the carbonate unit (−$CH_2$−O−C(O)−O−, $\delta$ = 4.25 ppm). $^{13}$C NMR spectra are also provided in **Figure S1** (ESI). These spectra show the characteristic resonances of the copolymers in agreement with our previous investigations carried out on homopolymers.[17,19] IR analysis also shows the presence of both cyclic and linear carbonates with the typical C=O band at 1800 $cm^{-1}$ for the cyclic one and at 1742 $cm^{-1}$ for the linear one (**Figure 2**). The presence of the ketone group is also observed for the polymers **P2**−**P5** by the characteristic band at 1720 $cm^{-1}$. The relative intensities of the two C=O bands of the two types of carbonates are in line with their relative content in the copolymer. The ratio of ether to carbonate (cyclic + linear) linkages is increased by the content of PEG introduced in the formulation, thus from 0 for **P1** to 45 for **P6**, and intermediate compositions for the other polymers (**Table 1**).

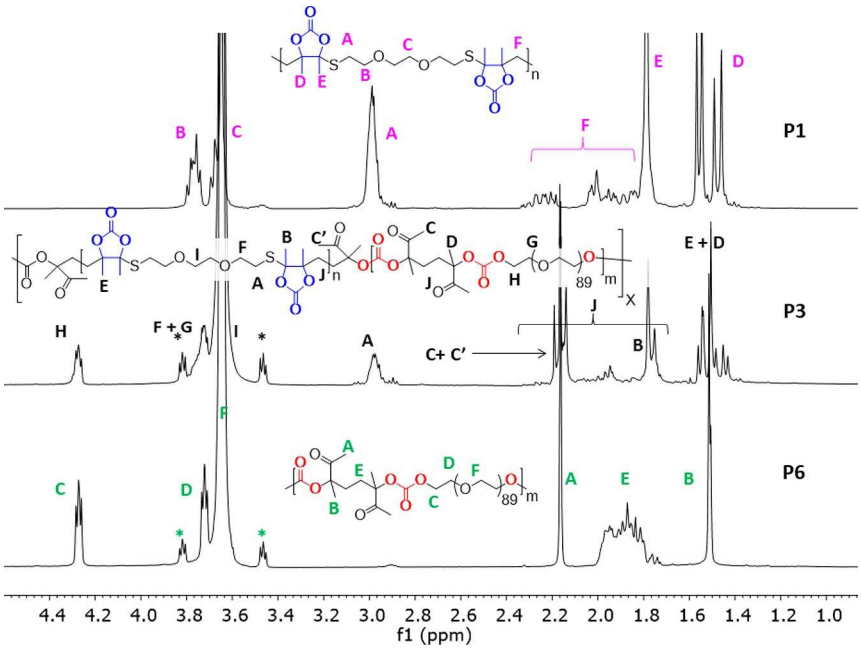


**Figure 1.** Stacked $^{1}$H NMR spectra of polymers **P1**, **P3**, and **P6** (**Table 1**).

*Published in : ASC Applied Polymer Materials (2020), vol. 2, n°2, pp. 922–931*
*DOI: 10.1021/acsapm.9b01130*
*Status : Postprint (Author's version)*

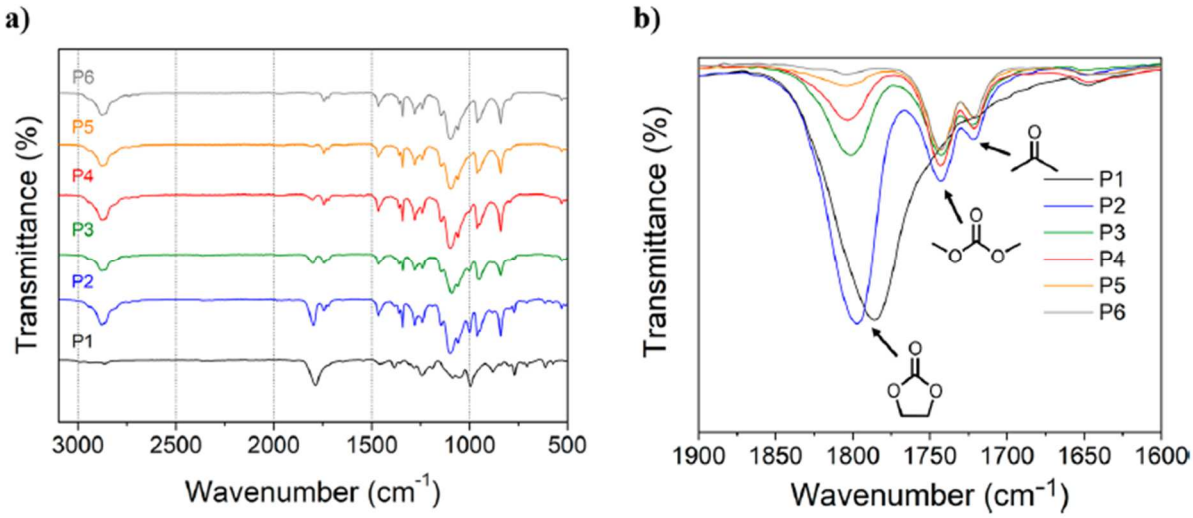


**Figure 2.** (a) FTIR spectra of polymers **P1**–**P6** and (b) zoom of the carbonyl region.

**Thermal Properties, Ionic Conductivity, and Lithium Diffusivity of the (Co)polymers.** The glass transition ($T_g$) and melting temperatures ($T_m$) of the polymers were evaluated by DSC. The DSC curves are shown in **Figure 3**a and the data are summarized in **Table 1**. Except for the homopolymer **P1**, all of the polymers are semicrystalline polymers ($T_m \approx 45$ °C). Nevertheless, it is not possible to determine the glass transition of the semicrystalline materials by the technique that was used. The homopolymer **P1** bearing the cyclic carbonate groups presents a glass transition temperature ($T_g$) of 43 °C with no crystallization peak. By adding LiTFSI from 10 to 50 wt %, $T_g$ is decreased to 42 and 10 °C, respectively, as the result of the plasticization effect of the salt (**Figure 3**b). This plasticization effect has already been analyzed by Tominaga et. al, where the highly concentrated polycarbonate-SPEs show low glass transition values.[20–22] This effect cannot be observed in the other SPEs due to the high EO unit content. In the absence of salt, the copolymers with different contents of cyclic carbonate groups (**P2**–**P5**) show a melting temperature ($T_m$) at 41–50 °C, that roughly corresponds to $T_m$ of the PEG segments (**Figure 3**a). Although a $T_m$ is still observed with 10 wt % of salt, the copolymers became completely amorphous for higher salt contents with $T_g$ values between −38 and −42 °C for salt contents of 30 wt % (**Figure 3**c, **Figure S2**). This observation contrasts the homopolymer of linear carbonate (**P6**) that presented a slight $T_m$ for this salt content.[9] In the case of **P1**– **P5**, increasing the salt content to 50 wt % does not drastically affect the $T_g$ value; in all cases, it is around −40 °C. Nevertheless, the homopolymer with only cyclic carbonate linkages (**P1**) holds a drastically higher glass transition value ($T_g$ = 32 °C containing 30 wt % LiTFSI) than for the copolymers with the same salt content (−35 °C < $T_g$ < −42 °C), indicating that the homopolymer is characterized by a lower chain mobility.

The ionic conductivity of all polymers (**P1**–**P5**) containing various contents of LiTFSI (10, 30, and 50 wt %) was then evaluated by EIS and the results are summarized in **Figure S3**. Except for the homopolymer of cyclic carbonate **P1**, in the case of the rest matrixes 30 wt % salt provided the highest ion conductivity over the whole temperature range that was investigated (25–90 °C). This optimal salt content is in agreement with previous studies on other polyether or polyester-based polycarbonates that showed that a 30–36 wt % LiTFSI composition provided the highest ionic conductivity value.[7,10,23,24]

*Published in : ASC Applied Polymer Materials (2020), vol. 2, n°2, pp. 922–931*
*DOI: 10.1021/acsapm.9b01130*
*Status : Postprint (Author's version)*

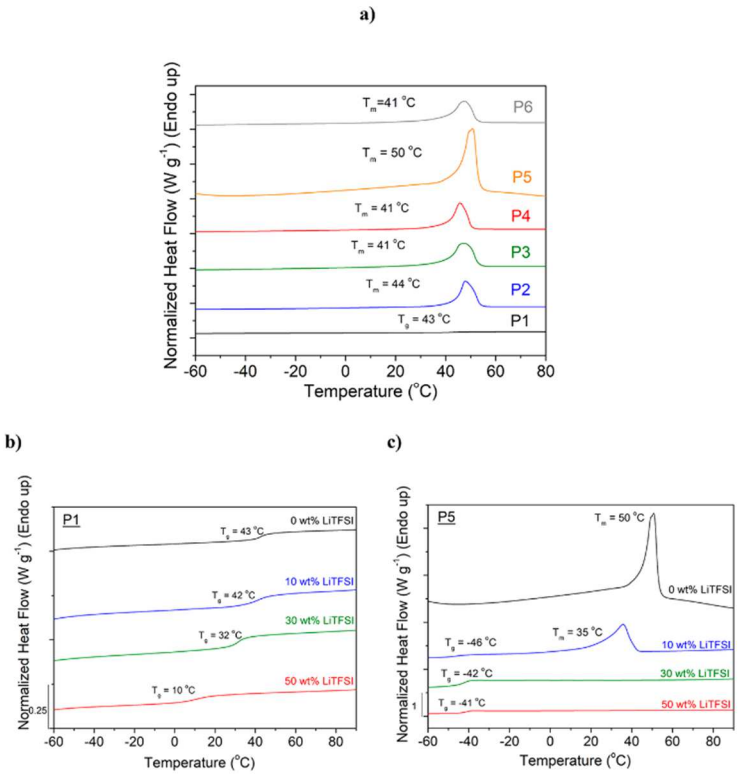


**Figure 3.** (a) DSC traces of the polymers **P1–P6** without LiTFSI; (b) DSC curves of **P1** with different content of LiTFSI; and (c) DSC curves of the polymers **P5** with different contents of LiTFSI. (DSC curves of **P2**, **P3**, and **P4** with different contents of LiTFSI are provided in SI, **Figure S2**.) All of the DSC data are recorded during the second heating scan.

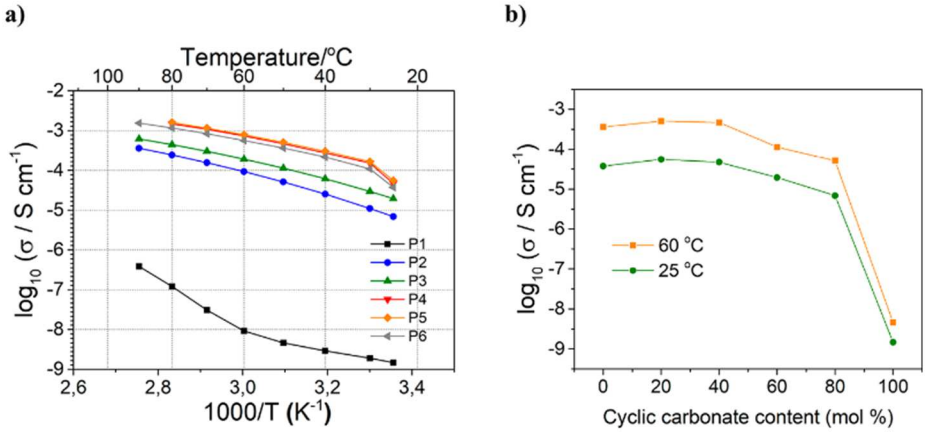


**Figure 4.** (a) Arrhenius plot, temperature dependence of the ionic conductivity of **P1–P6** in the presence of 30 wt % of LiTFSI (**P4** and **P5** conductivities almost overlay); (b) ionic conductivity of the polymers at 25 and 60 °C as a function of cyclic carbonate content in the presence of 30 wt % of LiTFSI

The ionic conductivity of all polymers (**P1**–**P5**), including the one bearing linear carbonate linkages only (**P6**),[17] containing 30 wt % LiTFSI were then compared at different temperatures (**Figure 4**a). All data are provided in Supporting Information (**Figure S4**). As expected, the ionic conductivity of the 100 mol % cyclic carbonate homopolymer **P1** is very low due to the poor mobility of the polymer chains. An important increase in ionic conductivity is observed when only 21 mol % of linear carbonate is incorporated in the polymer backbone (**P2**), confirming that the DSC results showed a significant

*Published in : ASC Applied Polymer Materials (2020), vol. 2, n°2, pp. 922–931*
*DOI: 10.1021/acsapm.9b01130*
*Status : Postprint (Author's version)*

decrease of $T_g$. The ionic conductivity still increases when the ratio in linear carbonate increases until leveling off above 64 mol % of linear carbonate (**Figure 4**b). These results show that about 40 mol % of cyclic carbonate does not significantly impact the ionic conductivity of the polymer. Importantly, the ion conductivity of the copolymer containing 18 mol % cyclic carbonate (**P5**) presents a conductivity of $7.9 \times 10^{-4}$ and $5.6 \times 10^{-5}$ S cm$^{-1}$ at 60 and 25 °C, respectively (**Figure 4**a,b). This ion conductivity is thus 424% and 150% higher than that measured for the homopolymer of linear carbonate **P6** ($1.86 \times 10^{-4}$ and $3.75 \times 10^{-5}$ S cm$^{-1}$ at 60 and 25 °C, respectively)[17] and higher or similar than most efficient PC-based SPEs.[7,10,25,26] These results indicate that the cyclic carbonates are able to enhance the ionic conductivity.

FTIR spectra of the polymers **P1–P5** with the different salt contents were then recorded, and the 1700−1900 cm$^{-1}$ range is highlighted in order to show any possible coordination of $Li^+$ to the cyclic carbonate (1800 cm$^{-1}$), linear carbonate (1742 cm$^{-1}$), and/or pendant ketone (1720 cm$^{-1}$) groups. In the case of coordination, a bathochromic shift of the carbonyl band is commonly observed.[7,13] **Figure 5** illustrates the FTIR spectra of two representative examples, **P1** and **P5**, and shows that this shift is only noted for high salt concentrations (50 wt % LiTFSI) to the cyclic carbonate group only. This observation is made for all polymers (see **Figure S5** for FTIR spectra of the other polymers) which suggests that lithium preferentially coordinates to cyclic carbonates among the different carbonyl groups. At lower salt concentration, it is not clear whether lithium cation coordinates to the carbonyl group or not, suggesting that it coordinates to ethylene oxide units. Nevertheless, if we compare these results with the ionic conductivity analysis at lower salt concentrations, it is evident that the ionic conductivity values are improved with the addition of the cyclic carbonate groups, even if it is not observed in the coordination in the FTIR analysis. At this stage, it is unclear how the cyclic carbonate affects the coordination of lithium.

$Li^+$ and $NTf_2^-$ diffusivity were measured by $^7$Li and $^{19}$F PFG-NMR in order to get insight into the mobility of both the cation and the anion of LiTFSI. **Figure 6** shows that both $^7$Li and $^{19}$F diffusion is slightly but systematically faster in **P5** than in **P3** at all the measured temperatures. This is consistent with conductivity data which show that **P5** has higher conductivity (**Figure 4**a). It is well-known that the ion diffusivities in polymer/salt composites are strongly influenced by polymer chain mobility.[27,28] Higher polymer chain, segments, or side chain mobility may facilitate ion migration within the composites. As such, the higher ion diffusivity in **P5** than **P3** may be attributed to the larger fraction of linear PC polymer chain which is of faster polymer chain mobility compared to the cyclic PC chain. Besides, it is also observed that $NTf_2^-$ diffuses much faster than the $Li^+$ in both samples. This may be related to the stronger interactions of $Li^+$/polymer compared to the $NTf_2^-$/polymer. This behavior is also frequently observed in conventional liquid electrolytes, which consist of lithium salts and ethylene carbonates and propylene carbonates, where the lithium ion is strongly coordinated to the solvent molecule and diffuses with it as an entity,[29] while the anion/solvent coordination is relatively weak and anions (florinated) exist relatively free.[30]

**Figure S7**a (Supporting Information) shows that both samples have quite similar T1 relaxation time for $^7$Li nucleus. However, the T1 minimum of **P3** shifted to higher temperature. The temperature dependency of the T1 relaxation can be well described by the Bloembergen– Purcell–Pound equation,[31] where the T1 relaxation time is extremely long at very low temperature, gradually decreases and goes through a minimum, and then rises up again with further increasing temperature. The minimum point of the curve represents the temperature at which the charactistic frequency of $^7$Li motion equals

*Published in : ASC Applied Polymer Materials (2020), vol. 2, n°2, pp. 922–931*
*DOI: 10.1021/acsapm.9b01130*
*Status : Postprint (Author's version)*

Larmor frequency, 116.6 MHz in this case. Therefore, the higher temperature shift of **P3** suggests a slightly slower ion dynamics compared to **P5**. This trend is more clearly seen in **Figure S7**b where **P3** has systematically longer correlation time, $\tau$, than **P5** at all temperatures, though their activation energy associated with the lithium ion dynamics is essentially identical. The lower ion dynamics of **P3** is also consistent with the slower diffusion coefficient obtained by PFG-NMR results shown in **Figure 6** as well as the lower conductivity shown in **Figure 4**.

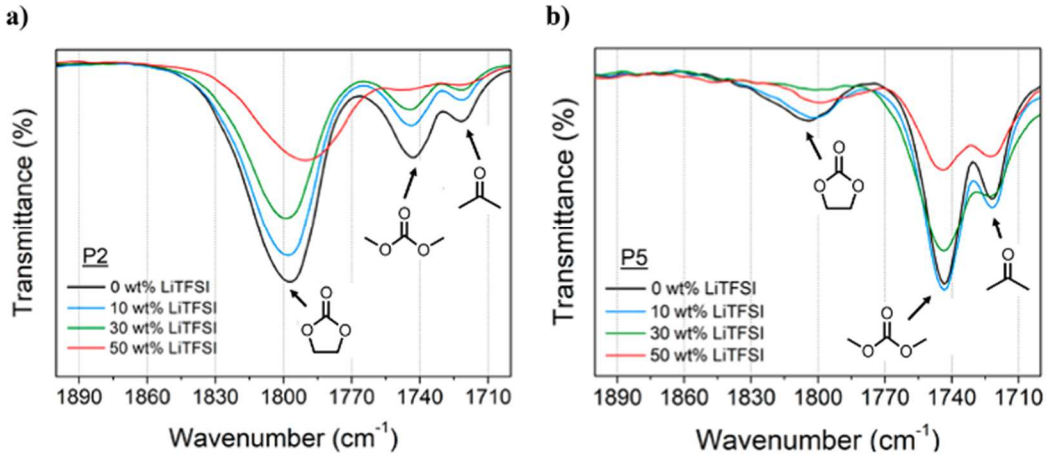


**Figure 5.** FTIR spectra (1700–1900 $cm^{-1}$) of the polymers (a) **P2** and (b) **P5** with different LiTFSI contents.

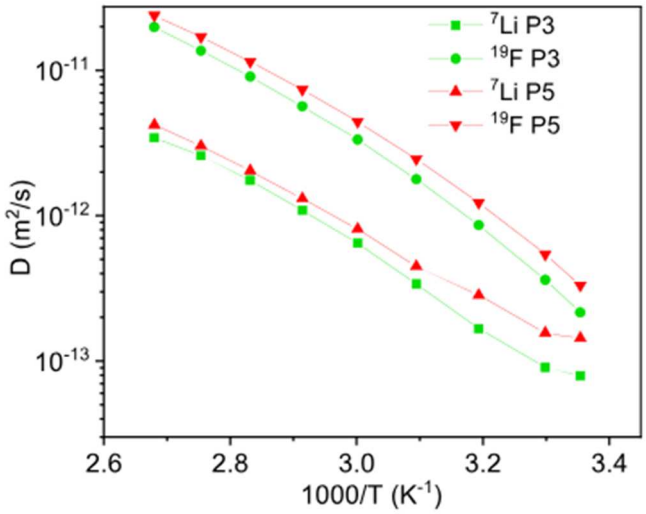


**Figure 6.** Arrhenius plot of $^{7}Li$ and $^{19}F$ diffusion coefficients of **P3** and **P5** samples.

*Published in : ASC Applied Polymer Materials (2020), vol. 2, n°2, pp. 922–931*
*DOI: 10.1021/acsapm.9b01130*
*Status : Postprint (Author's version)*

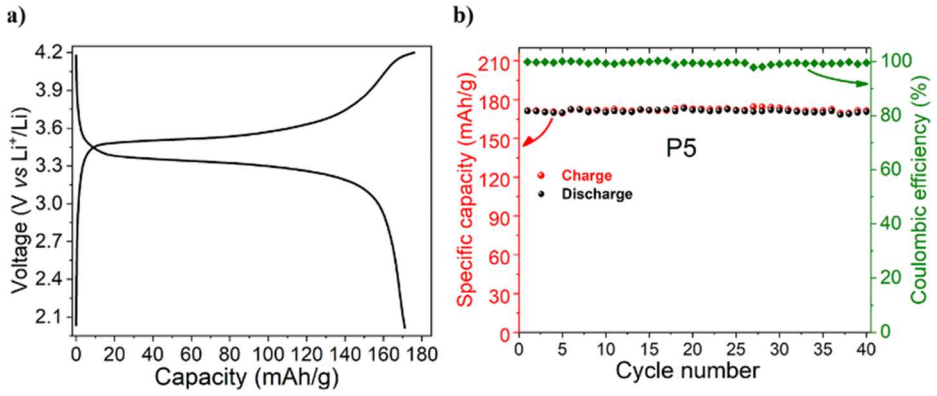


**Figure 7.** Electrochemical performance of the $LiFePO_4$/**P5**-based membrane/Li cell in the voltage range of 2.5−4.2 V at 60 °C. (a) First charge−discharge voltage profiles, (b) cycling performance at a current rate of 0.1 C (**P5**-based membrane: 58.4 wt % **P5**, 21 wt % LiTFSI, 14.8 wt % glass microfiber filter, 5.8 wt % TEG).

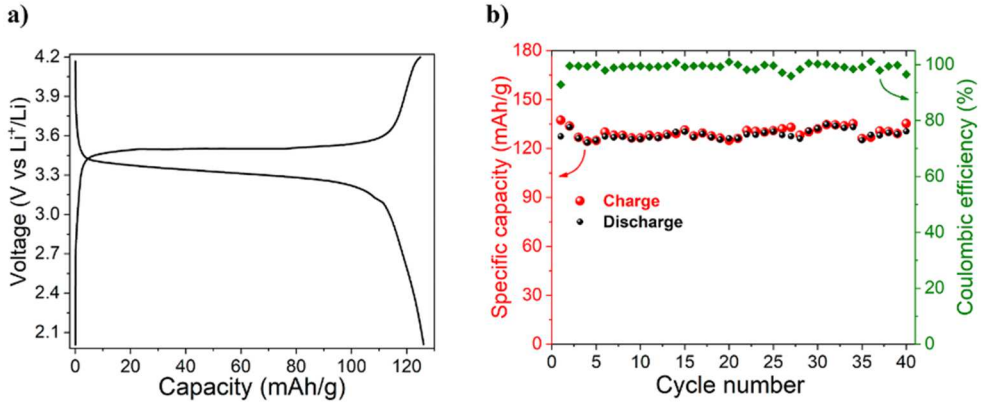


**Figure 8.** Electrochemical performance of the LiFePO 4/**P5**-based membrane/Li cell in the voltage range of 2.5−4.2 V at 25 °C. (a) Charge−discharge profiles, (b) cycling performance of the cell at a current rate of 0.1 C (**P5**-based membrane: 58.4 wt % **P5**, 21 wt % LiTFSI, 14.8 wt % glass microfiber filter, 5.8 wt % TEG).

**Preliminary Evaluation of the Polymers as Solid Electrolytes for Lithium Battery Application.** As the copolymer with 18 mol % of cyclic carbonate (**P5**) presents the most promising electrochemical properties, it has been selected for electrochemical stability and battery tests. The electrochemical stability window of **P5** containing 30 wt % LiTFSI was investigated by CV at 25 °C. **Figure S6** shows that its electrochemical stability is up to 5.6 V (vs $Li/Li^+$), compared to 5.2 V for our previously reported **P6**-based membrane.[17] Consequently, introducing cycling carbonate linkages seems to increase the electrochemical stability of the polymer, and **P5** appears as a promising SPE candidate for high voltage cathode materials of Li-ion batteries. Thermogravimetric analyses of **P5** and **P5** loaded with 30 wt % TFSI also show that the polymers are both thermally stable with a high degradation temperature at 10% ($T_{d(10\%)}$) of 353 and 367 °C, respectively (**Figure S8**).

Nevertheless, the copolymer does not form a self-standing membrane and can therefore not be used as a solid electrolyte as such without a separation membrane. In order to avoid the use of a membrane, we impregnated a Whatman glass microfiber filter with a solution of the polymer (7.8 wt %) in acetone containing LiTFSI (2.8 wt %) and tetraglyme (TEG, 0.8 wt %), followed by solvent evaporation (see **Experimental Section** for details). We added some TEG in the formulation because we previously

*Published in : ASC Applied Polymer Materials (2020), vol. 2, n°2, pp. 922–931*
*DOI: 10.1021/acsapm.9b01130*
*Status : Postprint (Author's version)*

demonstrated that the addition of this small quantity of high boiling point and nonflammable additive (10 wt % vs the all solid polymer) was enough to plasticize the polymer and to enhance the ion mobility at room temperature.[17] SEM images show that the polymer is impregnated in the entire thickness of the membrane (**Figure S9**) that is now self-standing with the following composition: 58.4 wt % **P5**, 21 wt % LiTFSI, 14.8 wt % glass microfiber filter, and 5.8 wt % TEG.

The electrochemical properties of the **P5**-based membrane in an all-solid-state lithium battery were then evaluated in coin cell by sandwiching this membrane between lithium metal as counter and reference material and lithium iron phosphate ($LiFePO_4$, LFP) as cathode material. Measurements were carried out at 25 and 60 °C in the potential range from 2.0 to 4.2 V. The specific capacity values are referred to the mass of LFP active material in the composite cathode. The charge−discharge voltage profile is represented in **Figure 7**a and the cycling performances of the Li/**P5**-based membrane/LFP obtained at 0.1 C and 60 °C are shown in **Figure 7**b. The Li/**P5**/LFP cell delivers a discharge capacity of 170 mAh $g^{-1}$ at 0.1 C which corresponds to the theoretical capacity of LFP (170 mAh $g^{-1}$). The typical voltage plateau at ∼3.35 V (vs $Li^+$/ Li) indicates that the **P5**-based electrolyte does not raise the cell polarization which is favorable for the Li-insertion/extraction into/from the grains of LFP active material during cycling. The observed plateau corresponds to the reversible electrochemical reaction, $LiFePO_4 \leftrightarrow FePO_4 + Li^+ + e^-$.

The cycling performance of the cell at a current density of 17 mA $g^{-1}$ (0.1 C) was measured at 60 °C during 40 cycles (**Figure 7**b). The Li/**P5**/LFP cell shows 100% of capacity retention and about 100% of Coulombic efficiency after 40 cycles. This result confirms that the **P5**-electrolyte presents very good stability and a high ionic conductivity under these conditions, thus at 60 °C.

In order to determine the influence of the cycling temperature on the **P5** electrochemical properties, Li/**P5**-based membrane/LFP cells were galvanostatically tested at room temperature (25 °C). **Figure 8**a presents the charge/ discharge curves of Li/**P5**-based membrane/LFP registered at 0.1 C (17 mA/g) in the potential window 2.0−4.2 V. The curves show the typical voltage profile reported for the LFP-material, and it is also similar to the charge/discharge curve of the material obtained at 60 °C with the same working voltage of around 3.35 V which corresponds to the $Fe^{2+}/Fe^{3+}$ redox couple.

This cell was also able to cycle at room temperature with a good initial discharge capacity of 125 mAh $g^{-1}$ at 0.1 C which corresponds to 73.5% of the theoretical capacity of LFP (170 mAh $g^{-1}$) with a capacity retention close to 100% after 40 cycles (**Figure 8**b). The lower specific capacity compared to the cycling performed at 60 °C is ascribed to the lower ionic conductivity of the **P5**-electrolyte at 25 °C, $5.6 \times 10^{-5}$ S $cm^{-1}$. However, the cell shows good performances at room temperature with excellent cycling stability with high retention capacity (∼100%) and Coulombic efficiency (∼99.7%), at least up to 40 cycles.

These cycling experiments clearly show that the capacity decreased by decreasing the cycling temperature. However, the working voltage corresponding to the $Fe^{2+}/Fe^{3+}$ redox couple remained similar either at room temperature or at 60 °C which confirms that the **P5** polymer does not raise the cell polarization even at room temperature which is favorable for lithium diffusion. The lower energy density obtained at room temperature is mainly due to the decrease of the specific capacity and not to the working voltage.

*Published in : ASC Applied Polymer Materials (2020), vol. 2, n°2, pp. 922–931*
*DOI: 10.1021/acsapm.9b01130*
*Status : Postprint (Author's version)*

In order to evidence the effect of TEG on the electrochemical performance of the device, we finally tested the cycling performance of the same device in the absence of TEG (all other components being identical). The cycling performances of $LiFePO_4$/non-TEG-doped **P5**-based membrane/Li cell were tested at 0.1 C at 60 °C. The evolution of charge/ discharge capacity and Coulombic efficiency versus cycle number is shown in the **Figure S10**. The first charge capacity was 170 mAh $g^{-1}$ that corresponds to the theoretical capacity of LFP material. However, the cell shows continuous decrease of the charge and discharge capacities leading to a capacity retention of 53% after 40 cycles with a relative Coulombic efficiency of ~90% during 40 cycles. This result could be due to the instability of the non-TEG-doped **P5**-based membrane and continuous lithium consumption during cycling.

# CONCLUSIONS

We have investigated the influence of the introduction of cyclic carbonate linkages within a polycarbonate/polyether backbone on the thermal properties and ion conductivity of polymers loaded with different contents of an organic salt (lithium bis(trifluoromethane) sulfonimide, LiTFSI). The polymers were produced in a one-pot process by the facile organocatalyzed polyaddition of a $CO_2$-based monomer (bis(*α*-alkylidene cyclic carbonate)) with poly(ethylene glycol) diol and a dithiol at room temperature. All polymers containing PEG segments presented a $T_m$ (characteristic of PEG segment) at around 41 °C and became amorphous with a low $T_g$ (around −40 °C) by loading them with 30 wt % LiTFSI. This is in sharp contrast to polymers containing cyclic carbonate linkages that are only characterized by a high $T_g$ (43 °C), even when loaded with 30 wt % LiTFSI ($T_g$ = 32 °C). The highest ion conductivity was measured for polymers containing a linear/cyclic carbonate linkages ratio of 82/18 with a value of $5.6 \times 10^{-5}$ S $cm^{-1}$ at 25 °C ($7.9 \times 10^{-4}$ S $cm^{-1}$ at 60 °C), which surpasses by 150% (424% at 60 °C) the conductivity measured for a similar polymer bearing linear carbonate linkages only. The introduction of only 18 mol % of cyclic carbonate linkages within the polymer backbone was thus enough to increase the ion conductivity, presumably due to the favorable coordination of lithium cation to the cyclic carbonate group as evidenced by FT-IR spectroscopy. This polymer was also characterized by a high oxidation stability up to 5.6 V (vs $Li/Li^+$). Because this polymer loaded with 30 wt % LiTFSI is a sticky material and has no mechanical resistance, it could not be used as a solid electrolyte alone. A self-standing solid electrolyte membrane was then constructed by impregnating a glass fiber filter by this optimal polymer, LiTFSI, and a small amount of a plasticizer (tetraglyme). We then assembled cells by sandwiching the membrane between a C-coated $LiFePO_4$ (LFP) as the cathode and lithium as the anode and counter electrode. The cycling performances were evaluated at 0.1 C and both at 60 °C and at room temperature for 40 cycles. Excellent cycling performances with capacity retention (~100%) were noted with 100% of the theoretical capacity (170 mAh $g^{-1}$) at 60 °C, and 73.5% of the theoretical capacity (125 mAh $g^{-1}$) at 25 °C. The cells were also cycling in the absence of TEG at 60 °C however they lacked long-term stability. This work illustrates the importance of the fine-tuning of the polymer structure for the optimization of the properties of the solid electrolyte.

*Published in : ASC Applied Polymer Materials (2020), vol. 2, n°2, pp. 922–931*
*DOI: 10.1021/acsapm.9b01130*
*Status : Postprint (Author's version)*

# ASSOCIATED CONTENT

## SUPPORTING INFORMATION

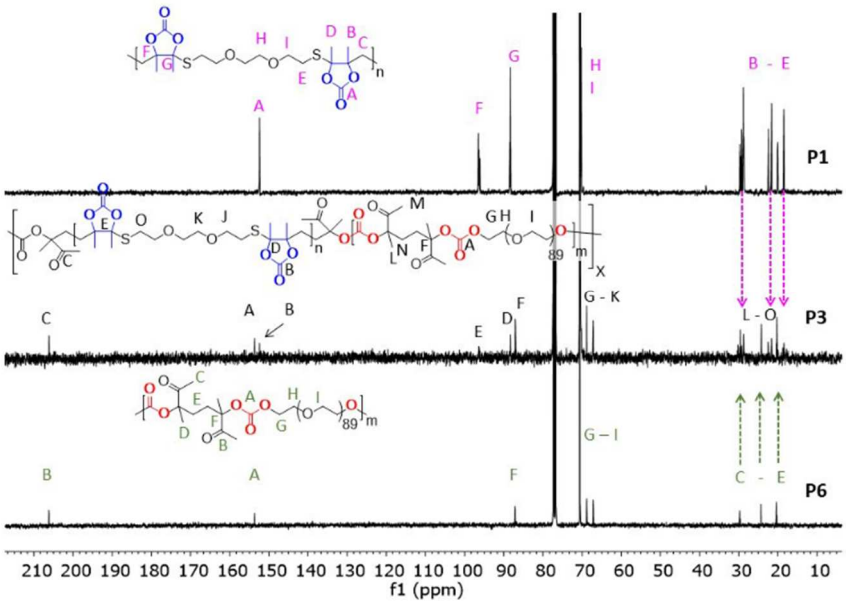


**Figure S1.** Stacked $^{13}C$ NMR spectra of polycarbonates **P1**-**P5** (**Table 1**) with different contents of cyclic and linear carbonates.

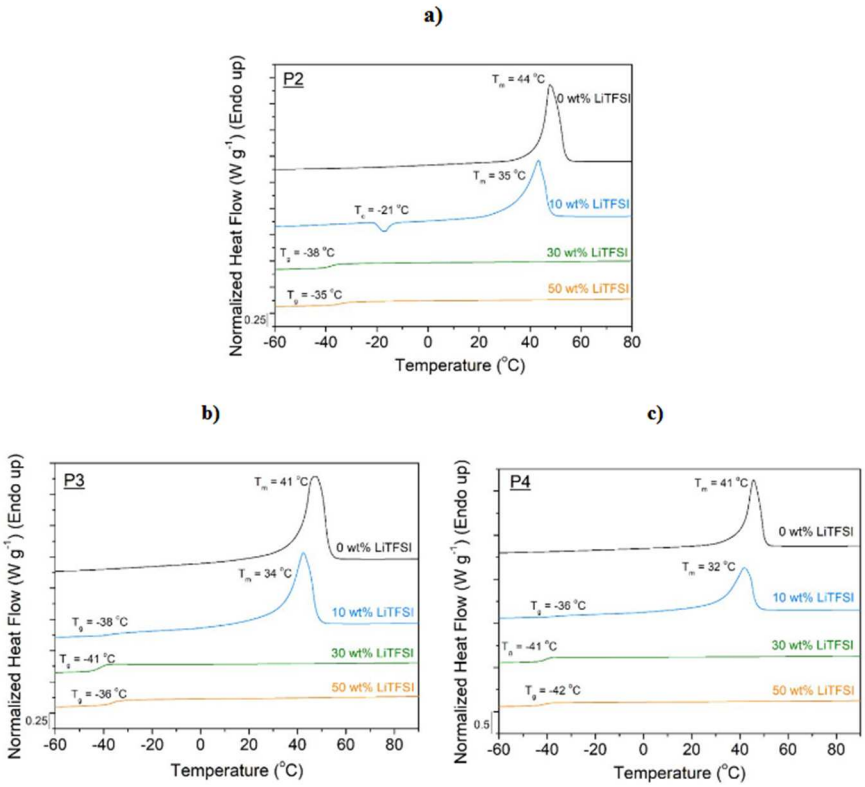


**Figure S2.** DSC curves of the polymers **P2**, **P3** and **P4** with different contents of LiTFSI. DSC data are recorded during the 2nd heating scan.

*Published in : ASC Applied Polymer Materials (2020), vol. 2, n°2, pp. 922–931*
*DOI: 10.1021/acsapm.9b01130*
*Status : Postprint (Author's version)*

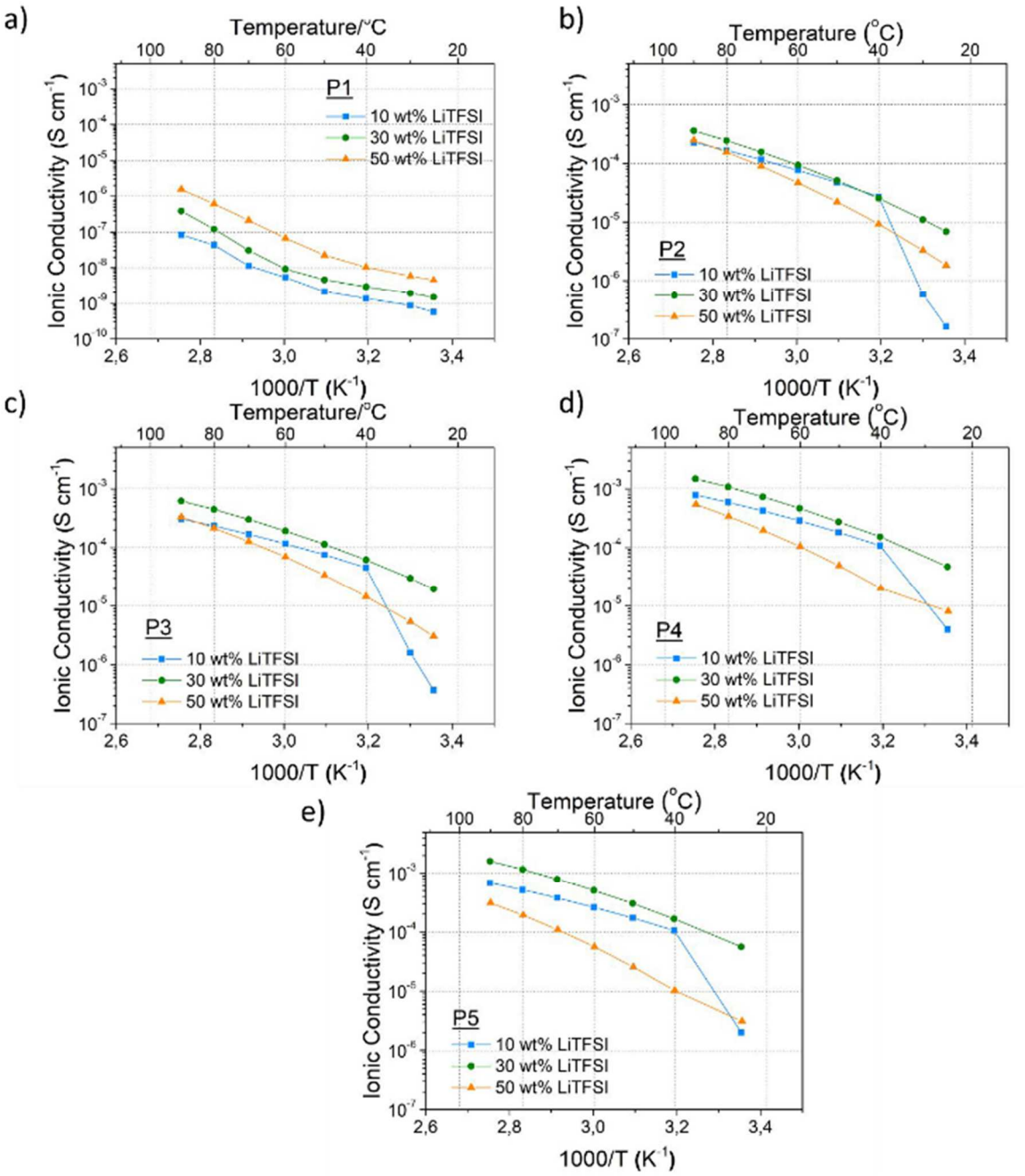


**Figure S3.** Arrhenius plot, temperature dependence of the ionic conductivity of the polymers with different cyclic/linear carbonate ratio in the presence of various contents of LiTFSI.

*Published in : ASC Applied Polymer Materials (2020), vol. 2, n°2, pp. 922–931*
*DOI: 10.1021/acsapm.9b01130*
*Status : Postprint (Author's version)*

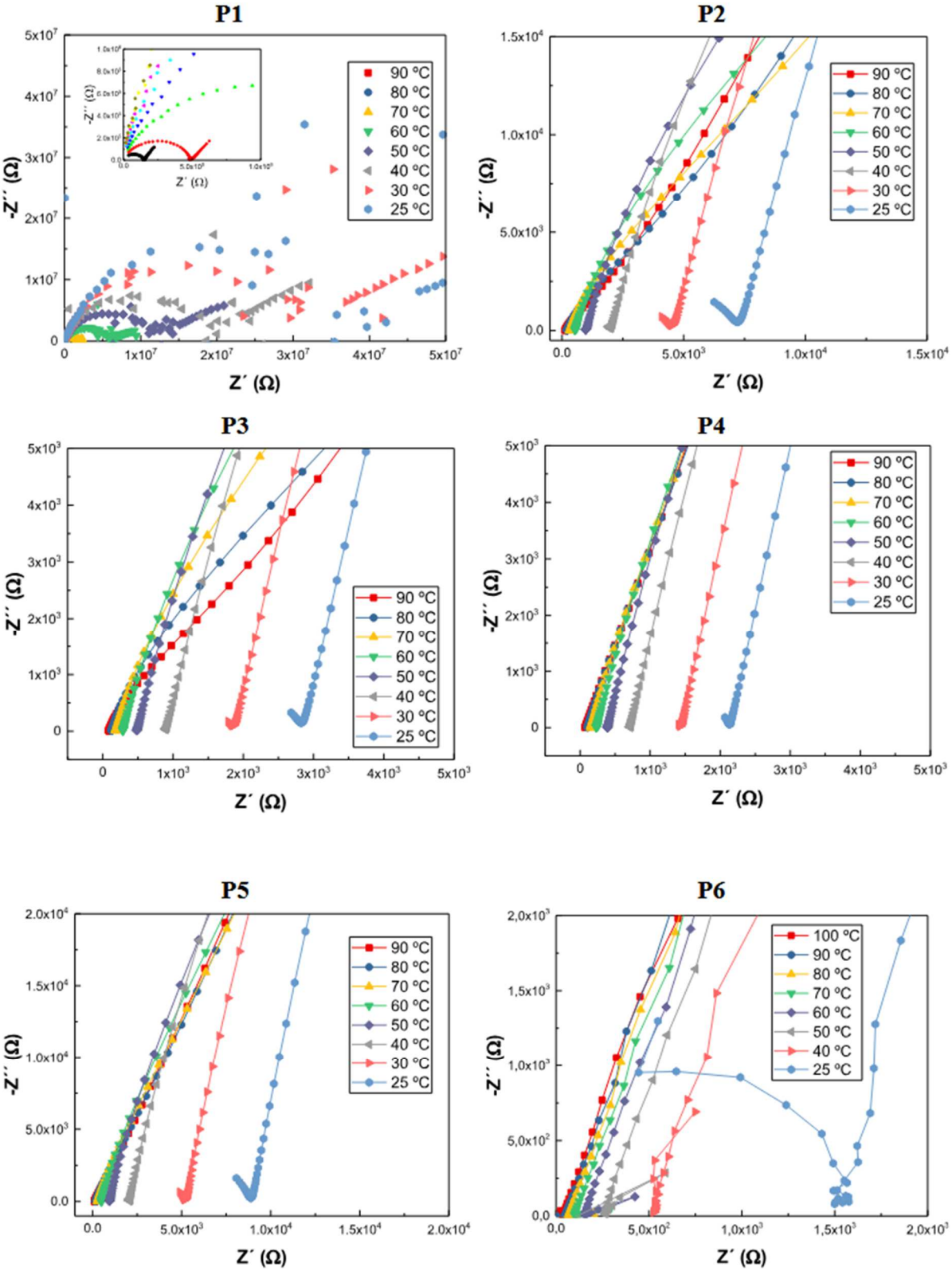


**Figure S4.** Comparative EIS studies (Nyquist plots) for the polymers loaded by 30 wt% LiTFSI. EIS data were collected in the 0.1 Hz to 0.1 MHz frequency range using a sinusoidal signal with an amplitude of 10 mV at equilibrium reduction peak potential.

*Published in : ASC Applied Polymer Materials (2020), vol. 2, n°2, pp. 922–931*
*DOI: 10.1021/acsapm.9b01130*
*Status : Postprint (Author's version)*

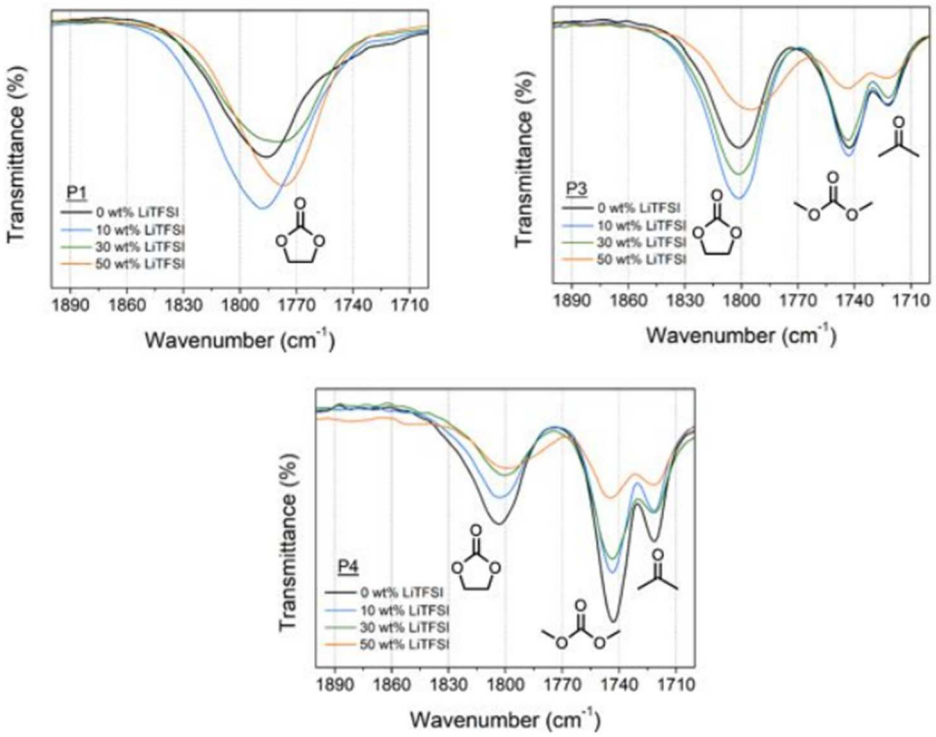


**Figure S5.** FTIR spectra (1700-1900 $cm^{-1}$) of the polycarbonates **P1**, **P3** and **P4** with different LiTFSI contents.

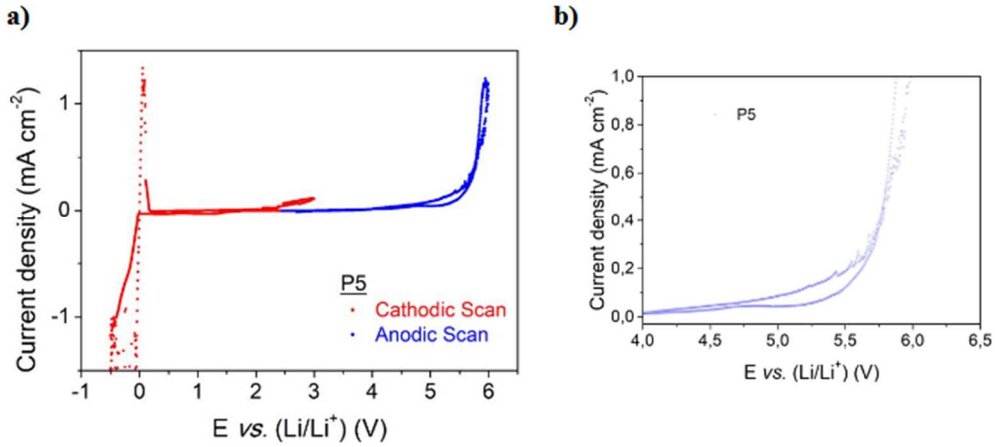


**Figure S6.** A) Electrochemical stability window of **P5** containing 30 wt% LiTFSI obtained by CV at a scan rate of 0.5 mV $s^{-1}$; b) zoomed electrochemical stability window of **P5** containing 30wt% LiTFSI.

*Published in : ASC Applied Polymer Materials (2020), vol. 2, n°2, pp. 922–931*
*DOI: 10.1021/acsapm.9b01130*
*Status : Postprint (Author's version)*

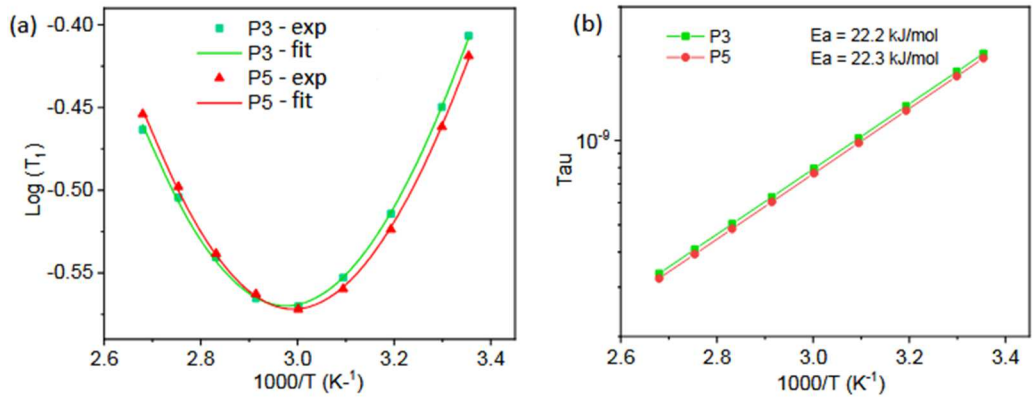


**Figure S7.** A) Bloembergen-Purcell-Pound (BPP) equation fitting of the $^{7}$Li T1 relaxation times of **P3** and **P5** samples; b) Arrhenius plot of the correlation times of both samples obtained from BPP fitting in (a).

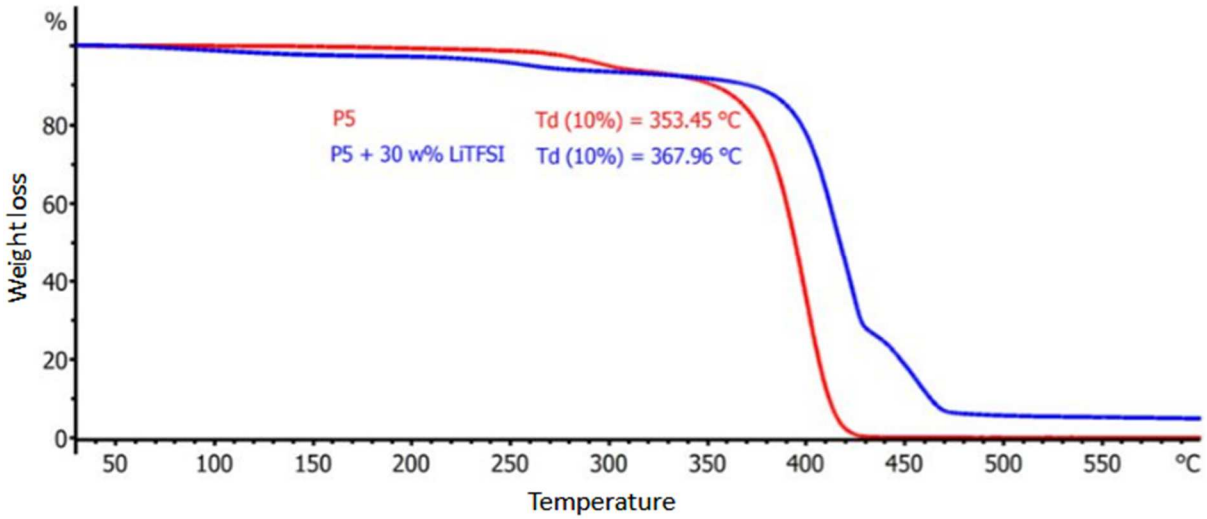


**Figure S8.** Thermogravimetric analyses of **P5** (red) and **P5** loaded with 30 wt% LiTFSI (blue) with a temperature ramp of 20°C/min.

*Published in : ASC Applied Polymer Materials (2020), vol. 2, n°2, pp. 922–931*
*DOI: 10.1021/acsapm.9b01130*
*Status : Postprint (Author's version)*

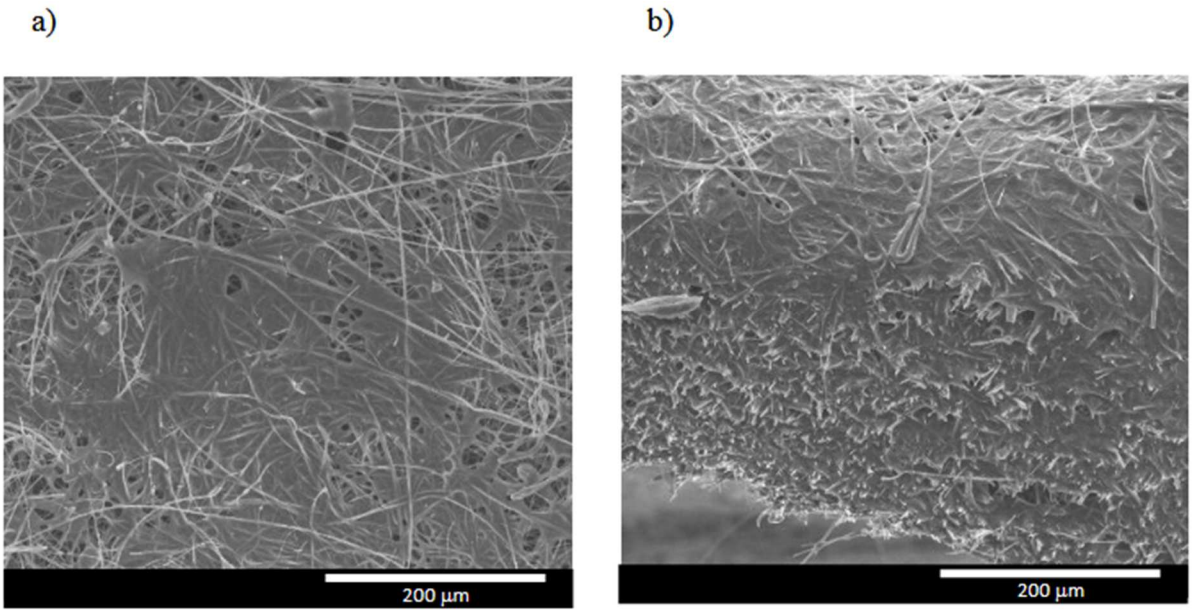


**Figure S9.** SEM micrographs of the membrane impregnated with the polymer a) surface of the membrane and b) cross section of the membrane (scale bar; 200µm).

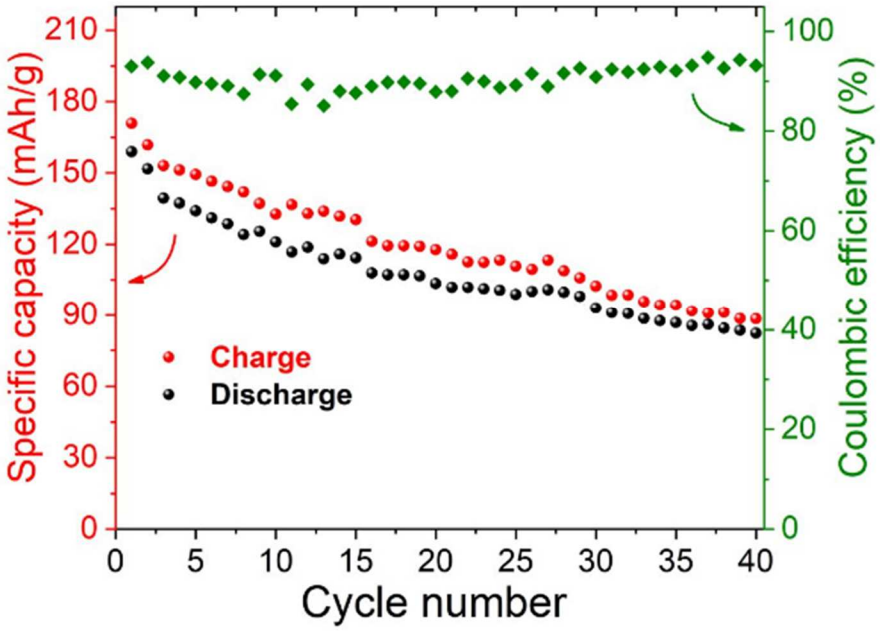


**Figure S10.** Cycling performance of the $LiFePO_4$/non-TEG-doped **P5**-based membrane /Li cell at a current rate of 0.1C at 60°C.

*Published in : ASC Applied Polymer Materials (2020), vol. 2, n°2, pp. 922–931*
*DOI: 10.1021/acsapm.9b01130*
*Status : Postprint (Author's version)*

# AUTHOR INFORMATION

**Corresponding Authors**

David Mecerreyes − POLYMAT, University of the Basque Country UPV/EHU, 20018 Donostia-San Sebastian, Spain;

Christophe Detrembleur − Centre for Education and Research on Macromolecules (CERM), CESAM Research Unit, University of Liege, Quartier Agora 4000, Liege, Belgium;

**Authors**

Farid Ouhib − Centre for Education and Research on Macromolecules (CERM), CESAM Research Unit, University of Liege, Quartier Agora 4000, Liege, Belgium

Leire Meabe − POLYMAT, University of the Basque Country UPV/EHU, 20018 Donostia-San Sebastian, Spain

Abdelfattah Mahmoud − GREENMAT-LCIS, Chemistry Department, University of Liege, Quartier Agora 4000, Liege, Belgium;

Bruno Grignard − Centre for Education and Research on Macromolecules (CERM), CESAM Research Unit, University of Liege, Quartier Agora 4000, Liege, Belgium

Jean-Michel Thomassin − Centre for Education and Research on Macromolecules (CERM), CESAM Research Unit, University of Liege, Quartier Agora 4000, Liege, Belgium

Frederic Boschini − GREENMAT-LCIS, Chemistry Department, University of Liege, Quartier Agora 4000, Liege, Belgium

Haijin Zhu − Institute for Frontier Materials (IFM), Deakin University, Waurn Ponds, VIC 3216, Australia

Maria Forsyth − Institute for Frontier Materials (IFM), Deakin University, Waurn Ponds, VIC 3216, Australia; Ikerbasque, Basque Foundation for Science, E-48011 Bilbao, Spain;

**Author Contributions**

[#]F.O. and L.M. contributed equally.

**Author Contributions**

The manuscript was written through contributions of all authors. All authors have given approval to the final version of the manuscript.

**Notes**

The authors declare no competing financial interest.

# ACKNOWLEDGMENTS

C.D. thanks the "Fonds National pour la Recherche Scientifique" (F.R.S.-FNRS) and the Fonds Wetenschappelijk Onderzoek − Vlaanderen (FWO) for financial support in the frame of the EOS project no. O019618F (ID EOS: 30902231). The authors from Liege thank the CESAM Research Unit for financial support. C.D. is F.R.S.-FNRS Research Director. D.M. and L.M. are grateful to the financial support of

the European Research Council by Starting Grant Innovative Polymers for Energy Storage (iPes) 306250 and the Proof of Concept Grant iPes-3DBat 789875. L.M. thanks Spanish Ministry of Education, Culture, and Sport for the predoctoral FPU fellowship received to carry out this work. The authors appreciate the technical and human support provided by SGIker of UPV/EHU for the NMR facilities of Gipuzkoa campus. A.M. and F.B. are grateful to the Walloon region for a Beware Fellowship Academia 2015-1, RESIBAT no. 1510399 and the support under "PE PlanMarshall2.vert" program (BATWAL − 1318146).

## ABBREVIATIONS

PC, polycarbonate ; LiTFSI , lithium bis-(trifluoromethanesulfonyl)imide; PEG, polyethylene glycol

## REFERENCES

(1) Fenton, D. E.; Parker, J. M.; Wright, P. V. Complexes of alkali metal ions with poly(ethylene oxide). *Polymer* 1973, 14 (11), 589.
(2) Armand, M. Polymer solid electrolytes - an overview. *Solid State Ionics* 1983, 9, 745−754.
(3) Armand, M. B. Polymer Electrolytes. *Annu. Rev. Mater. Sci.* 1986, 16 (1), 245−261.
(4) Armand, M. B.; Duclot, M. J.; Rigaud, P. Polymer solid electrolytes: Stability domain. *Solid State Ionics* 1981, 3, 429−430.
(5) Meyer, W. H. Polymer electrolytes for lithium-ion batteries. *Adv. Mater.* 1998, 10 (6), 439−448.
(6) Mindemark, J.; Lacey, M. J.; Bowden, T.; Brandell, D. Beyond PEO−Alternative host materials for Li+-conducting solid polymer electrolytes. *Prog. Polym. Sci.* 2018, 81, 114−143.
(7) Meabe, L.; Huynh, T. V.; Mantione, D.; Porcarelli, L.; Li, C.; O'Dell, L. A.; Sardon, H.; Armand, M.; Forsyth, M.; Mecerreyes, D. UV-cross-linked poly(ethylene oxide carbonate) as free standing solid polymer electrolyte for lithium batteries. *Electrochim. Acta* 2019, 302, 414−421.
(8) Tominaga, Y.; Yamazaki, K. Fast Li-ion conduction in poly(ethylene carbonate)-based electrolytes and composites filled with TiO2 nanoparticles. *Chem. Commun.* 2014, 50 (34), 4448−4450.
(9) Kimura, K.; Yajima, M.; Tominaga, Y. A highly-concentrated poly(ethylene carbonate)-based electrolyte for all-solid-state Li battery working at room temperature. *Electrochem. Commun.* 2016, 66, 46−48.
(10) Mindemark, J.; Sun, B.; Törmä, E.; Brandell, D. High-performance solid polymer electrolytes for lithium batteries operational at ambient temperature. *J. Power Sources* 2015, 298, 166−170.
(11) Berthier, C.; Gorecki, W.; Minier, M.; Armand, M.; Chabagno, J.; Rigaud, P. Microscopic investigation of ionic conductivity in alkali metal salts-poly (ethylene oxide) adducts. *Solid State Ionics* 1983, 11 (1), 91−95.
(12) Fergus, J. W. Ceramic and polymeric solid electrolytes for lithium-ion batteries. *J. Power Sources* 2010, 195 (15), 4554−4569.
(13) Mindemark, J.; Imholt, L.; Montero, J.; Brandell, D. Allyl ethers as combined plasticizing and crosslinkable side groups in polycarbonate-based polymer electrolytes for solid-state Li batteries. *J. Polym. Sci., Part A: Polym. Chem.* 2016, 54 (14), 2128−2135.
(14) Wei, X.; Shriver, D. F. Highly Conductive Polymer Electrolytes Containing Rigid Polymers. *Chem. Mater.* 1998, 10 (9), 2307−2308.
(15) Grignard, B.; Gennen, S.; Jérôme, C.; Kleij, A. W.; Detrembleur, C. Advances in the use of CO2 as a renewable feedstock for the synthesis of polymers. *Chem. Soc. Rev.* 2019, 48 (16), 4466−4514.
(16) Kamphuis, A. J.; Picchioni, F.; Pescarmona, P. P. CO2-fixation into cyclic and polymeric carbonates: principles and applications. *Green Chem.* 2019, 21 (3), 406−448.
(17) Ouhib, F.; Meabe, L.; Mahmoud, A.; Eshraghi, N.; Grignard, B.; Thomassin, J.-M.; Aqil, A.; Boschini, F.; Jérôme, C.; Mecerreyes, D.; Detrembleur, C. CO2-sourced polycarbonates as solid electrolytes for room temperature operating lithium batteries. *J. Mater. Chem. A* 2019, 7 (16), 9844−9853.

*Published in : ASC Applied Polymer Materials (2020), vol. 2, n°2, pp. 922–931*
*DOI: 10.1021/acsapm.9b01130*
*Status : Postprint (Author's version)*

(18) Gennen, S.; Grignard, B.; Tassaing, T.; Jérôme, C.; Detrembleur, C. CO2-Sourced α-Alkylidene Cyclic Carbonates: A Step Forward in the Quest for Functional Regioregular Poly(urethane)s and Poly(carbonate)s. *Angew. Chem.* 2017, 129 (35), 10530−10534.

(19) Ouhib, F.; Grignard, B.; Van Den Broeck, E.; Luxen, A.; Robeyns, K.; Van Speybroeck, V.; Jerome, C.; Detrembleur, C. A Switchable Domino Process for the Construction of Novel CO2-Sourced Sulfur-Containing Building Blocks and Polymers. *Angew. Chem.* 2019, 131 (34), 11894−11899.

(20) Tominaga, Y.; Yamazaki, K. Fast Li-ion conduction in poly(ethylene carbonate)-based electrolytes and composites filled with $TiO_2$ nanoparticles. *Chem. Commun.* 2014, 50, 4448−4450.

(21) Tominaga, Y.; Yamazaki, K.; Nanthana, V. Effect of Anions on Lithium Ion Conduction in Poly(ethylene carbonate)-based Polymer Electrolytes. *J. Electrochem. Soc.* 2015, 162 (2), A3133−A3136.

(22) Tominaga, Y.; Nanthana, V.; Tohyama, D. Ionic conduction in poly(ethylene carbonate)-basedrubbery electrolytes including lithium salts. *Polym. J.* 2012, 44, 1155−1158.

(23) Meabe, L.; Huynh, T. V.; Lago, N.; Sardon, H.; Li, C.; O'Dell, L. A.; Armand, M.; Forsyth, M.; Mecerreyes, D. Poly(ethylene oxide carbonates) solid polymer electrolytes for lithium batteries. *Electrochim. Acta* 2018, 264, 367−375.

(24) Meabe, L.; Lago, N.; Rubatat, L.; Li, C.; Müller, A. J.; Sardon, H.; Armand, M.; Mecerreyes, D. Polycondensation as a Versatile Synthetic Route to Aliphatic Polycarbonates for Solid Polymer Electrolytes. *Electrochim. Acta* 2017, 237, 259−266.

(25) Tominaga, Y.; Nakano, K.; Morioka, T. Random copolymers of ethylene carbonate and ethylene oxide for Li-Ion conductive solid electrolytes. *Electrochim. Acta* 2019, 312, 342−348.

(26) Tominaga, Y.; Shimomura, T.; Nakamura, M. Alternating copolymers of carbon dioxide with glycidyl ethers for novel ion-conductive polymer electrolytes. *Polymer* 2010, 51 (19), 4295−4298.

(27) Wang, X.; Chen, F.; Girard, G.; Zhu, H.; MacFarlane, D.; Mecerreyes, D.; Armand, M.; Howlett, P.; Forsyth, M. Poly(Ionic Liquid)s-in-Salt Electrolytes with Co-coordination-Assisted Lithium-Ion Transport for Safe Batteries. *Joule.* 2019, 3 (11), 2687−2702.

(28) Shubha, N.; Zhu, H.; Forsyth, M.; Srinivasan, M. Study of lithium conducting single ion conductor based on polystyrene sulfonate for lithium battery application. *Polymer* 2016, 99, 748−755.

(29) Ong, M.; Verners, O.; Draeger, E.; van Duin, A.; Lordi, V.; Pask, J. Lithium Ion Solvation and Diffusion in Bulk Organic Electrolytes from First-Principles and Classical Reactive Molecular Dynamics. *J. Phys. Chem.* B 2015, 119 (4), 1535−1545.

(30) Von Wald Cresce, A.; Gobet, M.; Borodin, O.; Peng, J.; Russell, S. M.; Wikner, E.; Fu, A.; Hu, L.; Lee, H.-S.; Zhang, Z.; Yang, X.-Q.; Greenbaum, S.; Amine, K.; Xu, K. Anion Solvation in Carbonate-Based Electrolytes. *J. Phys. Chem.* C 2015, 119 (49), 27255−27264.

(31) Bloembergen, N.; Purcell, E. M.; Pound, R. V. Relaxation Effects in Nuclear Magnetic Resonance Absorption. *Phys. Rev.* 1948, 73, 679−712.